ELSEVIER

Chemical Physics 246 (1999) 445–462

Chemical Physics

www.elsevier.nl/locate/chemphys

Fluorescence spectroscopic behaviour of neat and blended conjugated polymer thin films

W. Holzer [a], M. Pichlmaier [a], A. Penzkofer [a,*], D.D.C. Bradley [b], W.J. Blau [c]

[a] *Institut II - Experimentelle und Angewandte Physik, Universität Regensburg, D-93040 Regensburg, Germany*

[b] *Electronic and Photonic Molecular Materials Group, Department of Physics and Centre for Molecular Materials, The University of Sheffield, Hicks Building, Hounsfield Road, Sheffield S3 7RH, UK*

[c] *Department of Pure and Applied Physics, University of Dublin, Trinity College, Dublin 2, Ireland*

Received 12 January 1999

Abstract

The fluorescence quantum distributions, quantum yields, degrees of polarisation, and stimulated emission cross-section spectra of four *para*-phenylene vinylene and two *para*-phenylene ethynylene luminescent polymers were determined. Neat luminescent polymer films and polystyrene films doped with luminescent polymers were investigated. The fluorescence spectroscopic data analysis accounted for fluorescence absorption and reemission in thin films. The fluorescence spectroscopic behaviour of the solid thin films on fused silica substrates was compared with the corresponding behaviour of the luminescent polymers dissolved in liquid tetrahydrofuran.

Keywords: Fluorescence quantum yield; Luminescent polymers; Thin films; Fluorescence quantum distribution; Fluorescence polarisation

1. Introduction

Conjugated polymers have potential application in electro-luminescent optoelectronic devices [1,2]. They are used in light emitting diodes [3,4]. Lasing across the visible spectrum has been achieved using various fluorescent polymers in liquid [5–8] and solid [9,10] solution, in blended thin films using multiple scattering feedback [11], and in neat films employing microcavities [12–14], distributed feedback structures [15,16] and amplified spontaneous emission in waveguiding structures [17–24].

For thin-film lasing studies, an analysis of the fluorescence spectroscopic behaviour of the luminescent polymers in either neat or blended thin films is required. In this paper, we determined the fluorescence quantum distributions, quantum yields, degrees of fluorescence polarisation, and stimulated emission cross-section spectra of four *para*-phenylene vinylene and two *para*-phenylene ethynylene polymers. Neat thin films and blended polystyrene films were investigated. The fluorescent polymers studied showed laser oscillation in organic solvents such as tetrahydrofuran (THF) [7,8]. Laser generation (amplification of spontaneous emission,

* Corresponding author. Tel.: +49-941-943-2107; fax: +49-941-943-2754; e-mail: alfons.penzkofer@physik.uni-regensburg.de

0301-0104/99/$ - see front matter
PII: S0301-0104(99)00116-0

travelling wave lasing) was achieved in a polystyrene film and in a neat film for one of the luminescent polymers studied here (PBV-PPV 1,10, see below) [25]. The fluorescence characteristics of the investigated luminescent polymers in neat and blended films were compared with the fluorescence characteristics in THF [7,8,26–28].

The applied method of fluorescence quantum distribution and fluorescence quantum yield measurement is described in detail in Appendix A. It accounts for fluorescence absorption and fluorescence re-emission in bulk samples, in waveguiding thin films, and in non-waveguiding thin films on transparent substrates.

It should be noted that absolute internal fluorescence quantum distributions and absolute internal fluorescence quantum yields [29] were determined here in contrast to absolute external fluorescence quantum distributions and absolute external fluorescence quantum yields [29]. The absolute external fluorescence quantum yield is defined as the ratio of the total amount of fluorescence photons escaping the sample to the total amount of absorbed excitation photons. An integrating sphere is most useful for external fluorescence quantum yield measurements. The integrating sphere technique was applied to absolute external photoluminescence quantum efficiency measurements of luminescent polymer films in [30–32]. The true (internal or intrinsic) fluorescence quantum yield is defined as the ratio of emitted photons to absorbed photons by an infinitesimal volume element

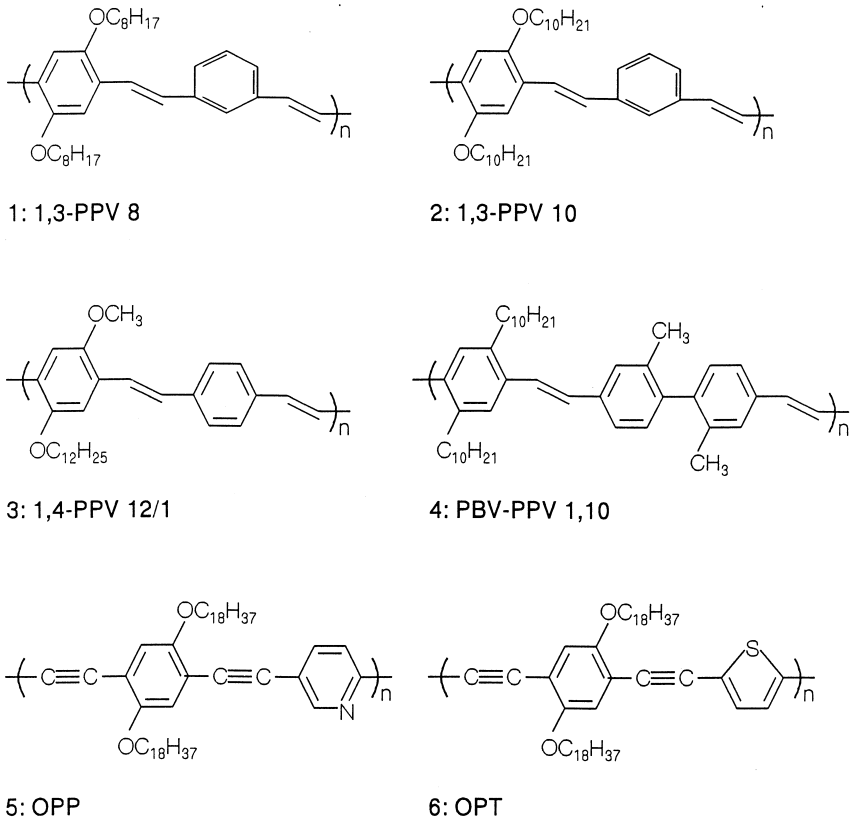

Fig. 1. Structural formulae of investigated luminescent polymers: (1) poly(*m*-phenylene vinylene-co-2,5-dioctoxy-*p*-phenylene vinylene) (1,3-PPV 8, monomeric molar mass $M_m = 406.7$ g mol^{-1}); (2) poly(*m*-phenylene vinylene-co-2,5-didecoxy-*p*-phenylene vinylene) (1,3-PPV 10, $M_m = 462.8$ g mol^{-1}); (3) poly(*p*-phenylene vinylene-co-2-methoxy-5-dodecoxy-*p*-phenylene vinylene) (1,4-PPV 12/1, $M_m = 418.6$ g mol^{-1}); (4) poly(2,2′-dimethyl-*p*-biphenyl-4-vinylene-co-2,5-didecyl-phenylene vinylene) (PBV-PPV 1,10, $M_m = 522.74$ g mol^{-1}); (5) poly(2,5-dioctadecyloxy-*p*-phenylene ethynylene-co-2,5-pyridinyl) (OPP, $M_m = 738.2$ g mol^{-1}); (6) poly(2,5-dioctadecyloxy-*p*-phenylene ethynylene-co-2,5-thienyl) (OPT, $M_m = 743.2$ g mol^{-1}).

inside the sample [29]. The external fluorescence quantum yield is smaller than the intrinsic fluorescence quantum yield because of fluorescence absorption (direct absorption and secondary absorption of internal reflected fluorescence light).

2. Experimental

The chemical structure formulae of the investigated polymers are shown in Fig. 1. The *para*-phenylene vinylene polymers (1,3-PPV 8, 1,3-PPV 10, 1,4-PPV 12/1, PBV-PPV 1,10) were synthesised at the Centre for Molecular Materials Group at the University of Sheffield [7] and the *para*-phenylene ethynylene polymers (OPP and OPT) were synthesised at the University of Dublin [8,33]. Polystyrene (molar mass 45000 g mol^{-1}) was purchased from Aldrich, Steinheim, Germany.

The neat thin polymer films on fused silica substrates were prepared by dissolving the polymers in THF (monomer units concentration of the order of 10^{-3} mol/dm^3) and casting them on fused silica substrates (size $50 \times 30 \times 3$ mm) [34]. The refractive index spectra and absorption coefficient spectra of the thin film polymers were determined previously [34]. The thickness of the neat films was determined by measuring the sample transmission at the fluorescence excitation wavelength and application of the Fresnel equations for a thin absorbing film on a thick transparent substrate [34,35].

The luminescent polymer doped polystyrene films on fused silica substrates (30 mm diameter and 2 mm thickness, apertured film area of 1×2 cm) were prepared by mixing 0.16 molar solutions of polystyrene in toluene with 1.5×10^{-3} molar luminescent polymer solutions in toluene and casting the mixture on the substrates. The number density ratio, $\kappa_{LP} = N_{LP}/N_{PS}$, where N_{LP} is the number density of luminescent polymer monomer units and N_{PS} is the number density of polystyrene monomer units in the solution, was in the region of 4×10^{-3} to 0.015 (see Table 3). The samples were dried at 90°C for 4 h. The relation between monomeric

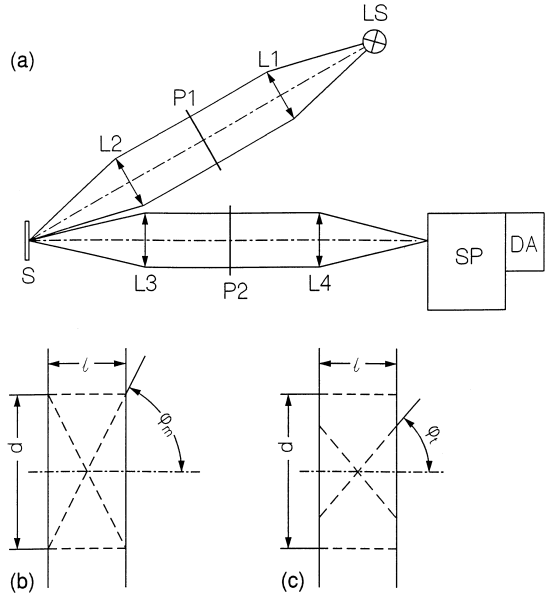

Fig. 2. (a) Experimental setup for fluorescence measurements. LS, light source (high pressure mercury lamp). L1–L4, lenses. P1, P2, polarisers. S, sample. SP, spectrometer. DA, diode-array detection system; (b) expanded cross-section of non-waveguiding sample; (c) expanded cross-section of waveguiding sample.

luminescent polymer concentration in polystyrene, C_{LP}, and the number density ratio, κ_{LP}, is given by $C_{LP} = \kappa_{LP} N_{PS}/N_A$, where N_A is Avogadro's number.

The thickness, ℓ, of the blended films at the local position of fluorescence measurement was determined by the neat transmission, $T'(\tilde{\nu}_L)$, measured at the fluorescence excitation wavelength, $\tilde{\nu}_L$. It is

$$T'(\tilde{\nu}_L) = T(\tilde{\nu}_L)/T_S(\tilde{\nu}_L) = \exp(-\alpha_L \ell), \tag{1}$$

where $T(\tilde{\nu}_L)$ is the transmittance of the blended film and the substrate, $T_S(\tilde{\nu}_L)$ is the transmittance of the blank substrate, and α_L is the absorption coefficient. α_L is given by

$$\alpha_L = \sigma_{L,m} N_{LP} = \sigma_{L,m} \kappa_{LP} N_{PS} = \sigma_{L,m} \kappa_{LP} \frac{N_A \rho_{PS}}{M_{PS}} = \sigma_{L,m} C_{LP} N_A, \tag{2}$$

where $\sigma_{L,m}$ is the monomeric absorption cross-section of the luminescent polymer at $\tilde{\nu}_L$, $\rho_{PS} = 1.05$ g cm^{-3} is the density [36], and $M_{PS} = 104.15$ g mol^{-1} is the monomeric molar mass of polystyrene. $\sigma_{L,m}$ is determined by

$$\sigma_{L,m} = \frac{\ln[T'(\tilde{\nu}_L)]}{\int_{S_0-S_1} \ln[T'(\tilde{\nu})]\,d\tilde{\nu}} \int_{S_0-S_1} \sigma_{a,m,THF}(\tilde{\nu})\,d\tilde{\nu}, \tag{3}$$

where it is assumed that the monomeric S_0–S_1 absorption cross-section integrals for the luminescent polymers in solution [$\sigma_{a,m,THF}(\tilde{\nu})$] and in film [$\alpha(\tilde{\nu})/N_{LP}$] are equal. This assumption is reasonable since the absorption integrals or oscillator strengths of allowed transitions depend little on solvent and concentration [37,38]. The

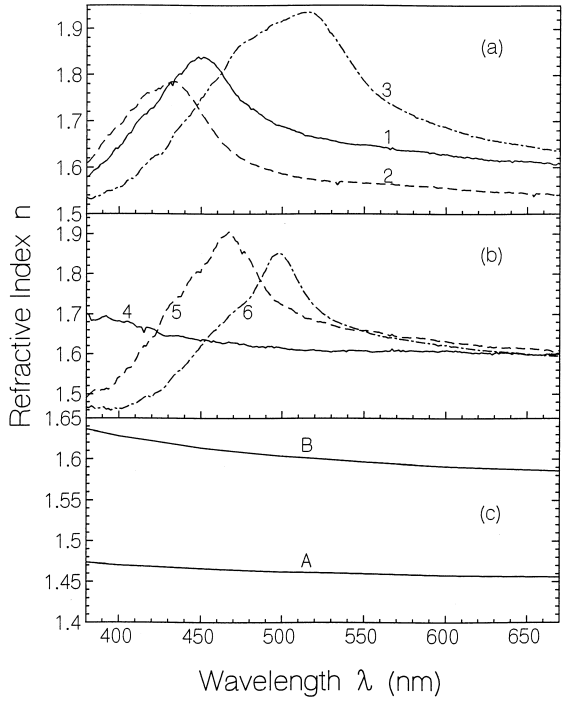

Fig. 3. (a) and (b) Refractive index spectra of neat thin films (from [34]). 1: 1,3-PPV 8. 2: 1,3-PPV 10. 3: 1,4-PPV 12/1. 4: PBV-PPV 1,10. 5: OPP. 6: OPT; (c) refractive index spectra of fused silica (A) and polystyrene (B). Refractive index data from [36] are interpolated using a single oscillator model [54].

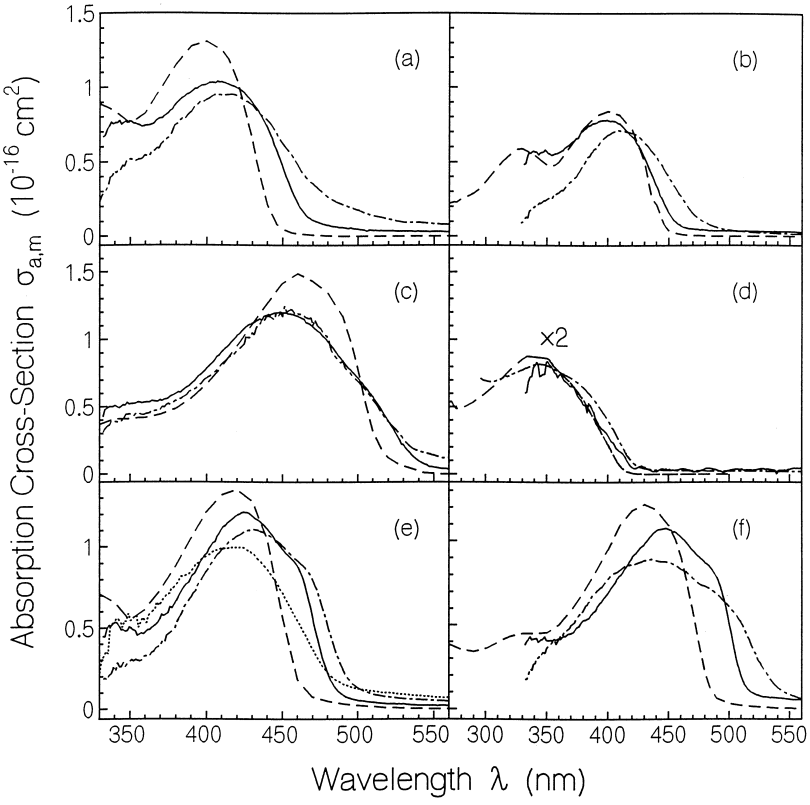

Fig. 4. Monomeric absorption cross-section spectra of neat thin films (solid curves), blended polystyrene films (dash-dotted curves, same concentration as in Fig. 5) and of luminescent polymers in THF (dashed curves, same concentration as in Fig. 5). (a) 1,3-PPV 8; (b) 1,3-PPV 10; (c) 1,4-PPV 12/1; (d) PBV-PPV 1,10 (curves are expanded a factor of two in vertical direction); (e) OPP; dotted curve, 7.2×10^{-4} molar OPP in polystyrene; (f) OPT. The liquid solution spectra of 1,3-PPV 8, OPP and OPT are taken from [28].

film thicknesses were additionally measured with a stylus profilometer (Dektak 3 from Sloan Technology, Santa Barbara, CA). A reasonable agreement between the stylus measurement and the thickness determination by transmittance measurement was found.

The fluorescence spectra were measured with a self-assembled fluorimeter [39]. The experimental arrangement is shown in Fig. 2. The fluorescence quantum distributions, $E_F(\lambda)$, were determined by vertical polarised excitation and magic angle detection (the polariser transmission axis was at an angle of 54.74° to the vertical direction of the excitation light [39,40]). For the calibration of the fluorescence quantum distribution, $E_F(\lambda)$, and the fluorescence quantum yield, ϕ_F, the polymer films were replaced by the organic dye Coumarin 314 T in ethanol of known fluorescence quantum yield ($\phi_R = 0.87$ [41]). The fluorescence quantum distributions and fluorescence quantum yields were calculated from the measured fluorescence spectra of the thin films and the reference dye including the effects of fluorescence absorption and fluorescence re-emission. The method of fluorescence analysis is described in Appendix A.

The fluorescence polarisation distribution [42,43]

$$P_F(\lambda) = \frac{E_{F,\parallel}(\lambda) - E_{F,\perp}(\lambda)}{E_{F,\parallel}(\lambda) + E_{F,\perp}(\lambda)} \tag{4}$$

Table 1
Selected S_0-S_1 absorption borders and absorption cross-section integrals

Luminescent polymer	Solvent						
	THF			neat film		PS	
	λ_a (nm)	λ_b (nm)	$\int_{S_0-S_1}\sigma_{a,m}(\tilde{\nu})d\tilde{\nu}$ (cm)	λ_a (nm)	λ_b (nm)	λ_a (nm)	λ_b (nm)
1,3-PPV 8	340	480	6.62×10^{-13}	355	530	345	600
1,3-PPV 10	340	500	4.32×10^{-13}	340	580	330	560
1,4-PPV 12/1	330	600	8.18×10^{-13}	330	600	330	670
PBV-PPV 1,10	270	450	3.91×10^{-13}	295	500	295	500
OPP	340	580	7.05×10^{-13}	345	600	330	670
OPT	340	560	6.96×10^{-13}	330	670	330	650

was determined by setting the polariser P1 (Fig. 2) to the vertical transmission direction and the polariser P2 to the vertical ($E_{F,\parallel}(\lambda)$) and horizontal ($E_{F,\perp}(\lambda)$) transmission positions.

3. Results

The refractive index spectra of the neat films are shown in Fig. 3(a) and 3(b) (from [34]). The refractive index spectra of the fused silica substrates (data from [36]), and of polystyrene (data from [36]) are shown in

Table 2
Absorption and emission spectroscopic data of investigated luminescent polymers

Sample	Solvent	ϕ_F	$P_F(\lambda_{F,max})$	$\tau_{rad,m}$ (ns)	$\tau_{F,m}$ (ns)	$\tau_{or,m}$ (ps)	$\lambda_{a,max}$ (nm)	$\lambda_{F,max}$ (nm)	$\delta\tilde{\nu}_{a,em}$ (cm^{-1})	$\Delta\tilde{\nu}_a$ (cm^{-1})	$\Delta\tilde{\nu}_{em}$ (cm^{-1})
1,3-PPV 8	neat	0.024	0.24	3.9	0.094	73	409	502	6000	~7300	4470
	PS	0.23	0.067	4.2	0.97	122	415	502	4300	~7100	4430
	THF	0.64	0.095	3.6	2.3	400	400	448	3600	~5600	3800
1,3-PPV 10	neat	0.043	0.29	7.7	0.33	380	400	488	5160	~6500	5070
	PS	0.44	0.15	7.4	3.2	1150	410	502	4590	~5000	4190
	THF	0.79	0.20	4.9	3.9	2170	400	445	3800	~5400	3500
1,4-PPV 12/1	neat	0.023	0.12	3.9	0.088	23	450	548	3970	6500	3450
	PS	0.25	0.19	3.9	0.98	505	455	517	2450	5900	2900
	THF	0.86	0.24	3.3	2.8	2150	460	510	2200	4700	2700
PBV-PPV 1,10	neat	0.40	0.10	6.4	2.6	530	350	466	7430	~10000	4700
	PS	0.64	0.36	6.3	4.1	870	348	443	6460	~11000	5100
	THF	0.75	0.37	5.2	3.9	9300	340	423	7000	10000	4150
OPP	neat	0.029	0.25	6.4	0.18	160	425	587	8100	5300	5170
	PS	0.12	0.28	3.9	0.48	505	432	453	2530	5300	7700
	THF	0.46	0.29	3.2	1.5	1730	420	457	1950	5000	2700
OPT	neat	0.043	0.074	5.6	0.24	35	447	556	5480	6100	5180
	PS	0.22	0.22	5.1	1.11	720	436	479	3370	8000	6140
	THF	0.40	0.21	3.5	1.4	510	430	485	2640	5600	2330

PS: polystyrene. THF: tetrahydrofuran. ϕ_F: fluorescence quantum yield. $P_F(\lambda_{F,max})$: degree of fluorescence polarisation at $\lambda_{F,max}$. $\tau_{rad,m}$: monomer radiative lifetime determined by Strickler–Berg formula (Eq. (5)). $\tau_{F,m}$: monomeric fluorescence lifetime. $\tau_{or,m}$: monomeric emission transition dipole moment reorientation time. $\lambda_{a,max}$: wavelength of peak S_0-S_1 absorption. $\lambda_{F,max}$: wavelength of maximum fluorescence quantum distribution. $\delta\tilde{\nu}_{a,em}$: spectral shift between S_0-S_1 absorption cross-section peak and stimulated emission cross-section peak. $\Delta\tilde{\nu}_a$: spectral width (FWHM) of absorption cross-section spectrum. $\Delta\tilde{\nu}_{em}$: spectral width of stimulated emission cross-section spectrum (FWHM).

Fig. 3(c). The refractive index spectra were needed for the calculation of the fluorescence quantum distributions (see Appendix A). For the blended films, the refractive index contribution of the luminescent polymers was neglected since the polystyrene content dominated ($\kappa_{LP} = N_{LP}/N_{PS} = 4 \times 10^{-3}$ to 0.015, see Table 3).

The monomeric absorption cross-section spectra, $\sigma_{a,m}(\lambda)$, of the neat films (solid curves), the blended polystyrene films (dash-dotted curves), and THF solutions (dashed curves) are displayed in Fig. 4(a), Fig. 4(b), Fig. 4(c), Fig. 4(d), Fig. 4(e), Fig. 4(f). The absorption cross-section spectra of the luminescent polymers in THF were determined by transmission measurements with a spectrophotometer. The absorption cross-sections of the neat thin films are taken from [34], where the optical constants, $n(\lambda)$, $\alpha(\lambda)$, and the film thickness, ℓ, were determined from reflectance and transmittance measurements. The absorption cross-section spectra, $\sigma_{a,m}(\lambda)$, were obtained by equating the S_0–S_1 absorption cross-section integrals, $\int \sigma_{a,m}(\tilde{\nu}) d\tilde{\nu}$, of the neat films and the THF solutions. The absorption cross-section spectra of the luminescent polymers in polystyrene were determined by transmission measurement ($T'(\tilde{\nu})$, Eq. (1)) and equating the polystyrene film and THF solution S_0–S_1 absorption cross-section integrals (Eq. (3)). The applied wavelength borders, λ_a and λ_b, of S_0–S_1 absorption and the determined S_0–S_1 absorption cross-section integrals in THF are listed in Table 1.

The wavelength positions, $\lambda_{a,max}$, of peak absorption in the S_0–S_1 transition region and the spectral half-width, $\Delta\tilde{\nu}_a$, of the S_0–S_1 absorption bands are listed in Table 2.

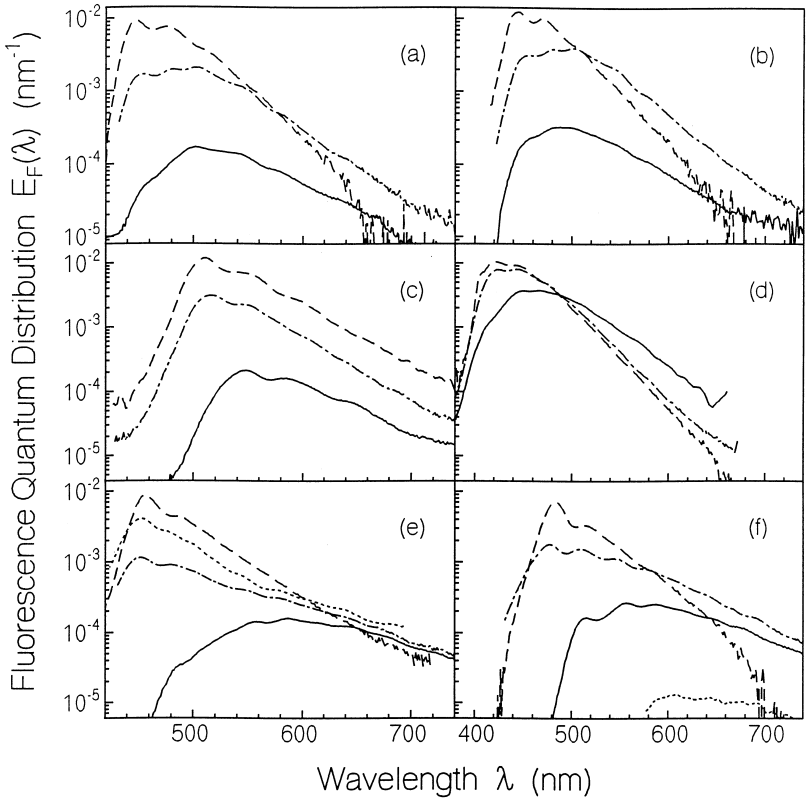

Fig. 5. Fluorescence quantum distribution, $E_F(\lambda)$, of neat thin films (solid curves), of polystyrene blended films (dash-dotted curves) and of luminescent polymers in THF (dashed curves). Sample parameters are given in Table 3. (a) 1,3-PPV 8; (b) 1,3-PPV 10; (c) 1,4-PPV 12/1; (d) PBV-PPV 1,10; (e) OPP; dotted curve, 7.2×10^{-4} molar OPP in polystyrene, $\ell = 230$ μm. (f) OPT; dotted curve, neat rhodamine 6G film.

The long-wavelength parts of the absorption cross-section spectra influence the fluorescence quantum distribution determination by the effect of fluorescence light absorption (see Appendix A). The S_0–S_1 absorption cross-section spectra are needed for the calculation of the stimulated emission cross-section spectra, $\sigma_{em,m}(\lambda)$, [44] (see Eq. (8) below).

The fluorescence quantum distributions, $E_F(\lambda)$, of the investigated samples are presented in Fig. 5. The fluorescence quantum yields, $\phi_F = \int_{S0-S1} E_F(\lambda)d\lambda$, are listed in Table 2. The highest fluorescence quantum yields were obtained for the luminescent polymers in liquid solution. In the polystyrene films, ϕ_F was reduced by roughly a factor of two compared to the liquid solutions. For the neat films, the fluorescence quantum efficiency was low ($\phi_F \approx 0.023$ for 1,4-PPV 12/1 to $\phi_F \approx 0.043$ for 1,3-PPV 10 and OPT) with the exception of PBV-PPV 1,10 where $\phi_F \approx 0.4$ was measured.

The wavelength positions, $\lambda_{F,max}$, of peak fluorescence emission are included in Table 2. The shifts of the emission peak to longer wavelengths were mostly in the order $\lambda_{F,max}(THF) < \lambda_{F,max}(PS) < \lambda_{F,max}$(neat film). The shifts were in the range of 38 nm for 1,4-PPV 12/1 to 130 nm for OPP between liquid solutions and neat films. The spectral half widths, $\Delta\tilde{\nu}_F$, of the fluorescence spectra, $E_F(\lambda)$, were broadened mostly in the order $\Delta\tilde{\nu}_F(THF) < \Delta\tilde{\nu}_F(PS) < \Delta\tilde{\nu}_F$(neat film). They were narrower than the spectral-half-widths of the S_0–S_1 absorption spectra, $\Delta\tilde{\nu}_a$ (see Table 2). Spectral humps are resolved both in the blended films and the neat films.

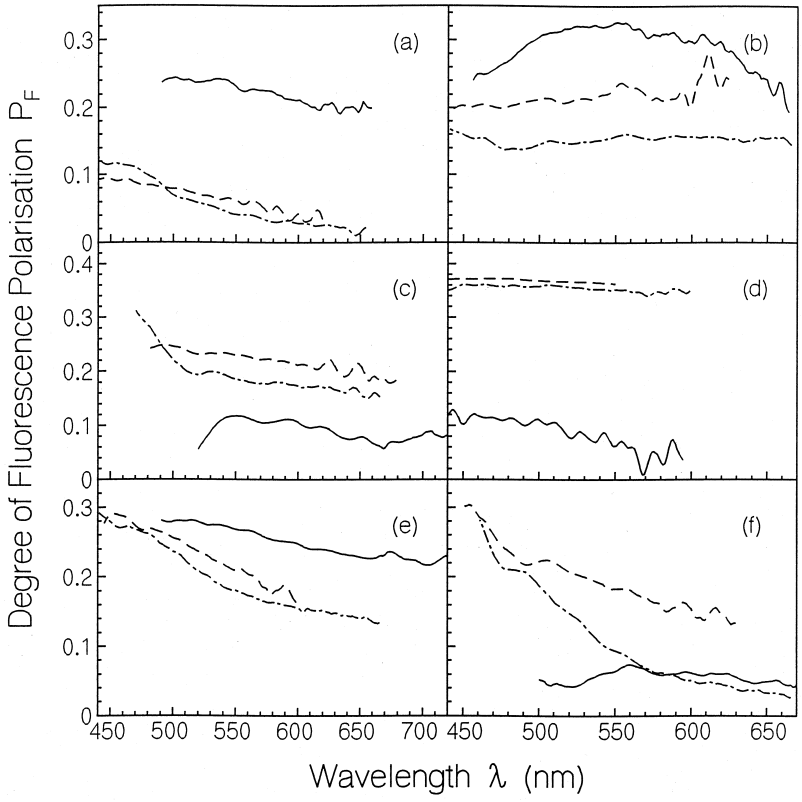

Fig. 6. Spectra of degree of fluorescence polarization, $P_F(\lambda)$, of investigated luminescent polymers. Sample parameters are given in Table 3. (a) 1,3-PPV 8; (b) 1,3-PPV 10; (c) 1,4-PPV 12/1; (d) PBV-PPV 1,10; (e) OPP; (f) OPT.

The monomeric radiative lifetime [28], $\tau_{rad,m}$, may be calculated from the fluorescence quantum distribution, $E_F(\lambda)$, and the monomeric absorption cross-section spectrum, $\sigma_{a,m}(\lambda)$, using the Strickler–Berg formula [45,46]

$$\frac{1}{\tau_{rad,m}} = 8\pi c_0 \frac{\int_{em} n^3(\lambda) E_F(\lambda) d\lambda}{\int_{em} E_F(\lambda) \lambda^3 d\lambda} \int_{abs} \frac{\sigma_{a,m}(\lambda)}{n(\lambda)\lambda} d\lambda, \quad (5)$$

where c_0 is the vacuum light velocity, and the integration runs over the $S_1 \rightarrow S_0$ emission range (em) and the $S_0 \rightarrow S_1$ absorption range (abs).

Values of $\tau_{rad,m}$ are listed in Table 2. It should be noted that the true radiative lifetime, τ_{rad}, of an emitting chromophore depends on the chromophore size (exciton size) which may extend over m_e monomers, leading to $\tau_{rad} = \tau_{rad,m}/m_e$ [28].

The monomeric fluorescence lifetime, $\tau_{F,m}$, is given by

$$\tau_{F,m} = \phi_F \tau_{rad,m}. \quad (6)$$

Determined values of $\tau_{F,m}$ are listed in Table 2. The true fluorescence lifetime of an emitting chromophore is given by $\tau_F = \tau_{F,m}/m_e$ [28]. Values of the emitting chromophore size, $m_e = \tau_{F,m}/\tau_F$, of 1,3-PPV 8 ($m_e \approx 1.5$), OPP ($m_e \approx 1.8$), and OPT ($m_e \approx 1.5$) were determined by separate time-resolved measurements of the fluorescence lifetime [28].

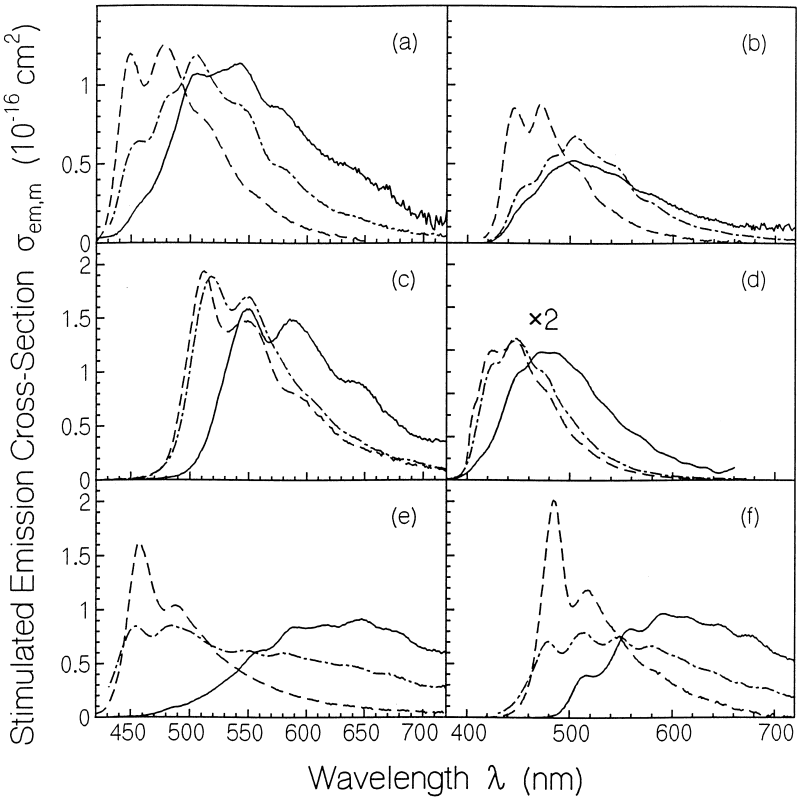

Fig. 7. Monomeric stimulated emission cross-section spectra, $\sigma_{em,m}(\lambda)$, of investigated luminescent polymers. Sample parameters are given in Table 3. (a) 1,3-PPV 8; (b) 1,3-PPV 10; (c) 1,4-PPV 12/1; (d) PBV-PPV 1,10; (e) OPP; (f) OPT.

The fluorescence polarisation spectra of the investigated luminescent polymer samples are shown in Fig. 6. Degrees of fluorescence polarisation, $P_F(\lambda_{F,max})$, at the wavelength of maximum fluorescence emission are listed in Table 2. In most cases, some decrease of fluorescence polarisation with increasing wavelength was observed.

The transition dipole moment reorientation time, τ_{or}, may be estimated roughly from the degree of fluorescence polarisation, P_F, and the fluorescence lifetime, τ_F, by the relation [47,48]

$$\tau_{or} = \frac{1/P_0 - 1/3}{1 - P_F/P_0} P_F \tau_F, \tag{7}$$

where P_0 is the degree of fluorescence polarisation in the absence of reorientation of the emitting transition dipole moment. ($P_0 = 0.5$ if the absorbing and the emitting transitions are the same, e.g. S_0–S_1 absorption and emission; this situation is considered here). Calculated monomeric reorientation times, $\tau_{or,m}$, are listed in Table 1. They are determined by using Eq. (7) with $P_0 = 0.5$, $P_F = P_F(\lambda_{F,max})$, and $\tau_F = \tau_{F,m}$. The true reorientation times are $\tau_{or} = \tau_{or,m}/m_e$ [28].

The monomeric stimulated emission cross-section spectra, $\sigma_{em,m}(\lambda)$, are obtained from the absorption cross-section spectra, $\sigma_{a,m}(\lambda)$, and the fluorescence quantum distributions, $E_F(\lambda)$, by the relation [44]

$$\sigma_{em,m}(\lambda) = \frac{\lambda^4 n(\lambda) E_F(\lambda)}{\int_{em} \lambda'^3 E_F(\lambda') d\lambda'} \int_{\lambda_a}^{\lambda_b} \frac{\sigma_{a,m}(\lambda')}{n(\lambda')\lambda'} d\lambda', \tag{8}$$

where em indicates the integration over the $S_1 \rightarrow S_0$ fluorescence emission region, and λ_a and λ_b are the wavelength borders of S_0–S_1 absorption (see Table 1).

The obtained monomeric stimulated emission cross-section spectra of the investigated samples are displayed in Fig. 7. The spectral shapes are similar to the fluorescence quantum distribution shapes since $\sigma_{em,m}(\lambda) \propto \lambda^4 E_F(\lambda)$, only the long-wavelength parts are increased because of the λ^4 dependence.

4. Discussion

The neat thin film, blended thin film, and the THF solution results are compared.

The neat and blended thin film absorption cross-section spectra are generally slightly shifted to longer wavelengths and they are spectrally broadened compared to the THF solution spectra. The film absorption spectra are partly more structured in the long-wavelength absorption part than the liquid THF absorption spectra. In THF solutions, the luminescent polymer concentration was in the region of 2.3×10^{-5} mol/dm^3 (1,3-PPV 8) to 1.3×10^{-3} mol/dm^3 (2,4-OPPV) (see Table 3). The polymer chains were well separated without interpolymer interaction [29,49,50]. For the blended films, the luminescent polymer concentration was in the range of 0.039 mol/dm^3 $\leq C_{LP} \leq$ 0.15 mol/dm^3, leading to an average polymer distance of $a_{LP} \approx (N_{LP}/m_{pol})^{-1/3} = (C_{LP} N_A/m_{pol})^{-1/3}$ in the range of 8 nm to 12 nm assuming an average degree of polymerisation of $m_{pol} = 50$. The polymer diameter in an ideal random walk model (good polymer solvent) [51] is $d_{LP} = m_{pol}^{1/2} b \approx 10$ nm to 15 nm using $m_{pol} \approx 50$ and a monomer length of $b \approx 1.5$ nm to 2 nm. Since the average polymer separation a_{LP} is less than or approximately equal to the ideal polymer diameter d_{LP}, an interaction between luminescent polymer chains occurs. The similarity of the blended and neat film spectra confirms a luminescent polymer–luminescent polymer interaction in the blended polymer films as it is present in the neat luminescent films.

In Fig. 4(e), the absorption cross-section spectrum of 7.2×10^{-4} molar OPP in polystyrene is included (dotted curve). Its spectral shape is unstructured like the spectrum of diluted OPP in THF, but it is broadened compared to the THF solution. Polystyrene is thought to be a good solvent for OPP and the other investigated

Table 3
Sample parameters applying to Figs. 5–7. Concentration of neat polymers is determined by $C_{LP} = \rho / M_m$, where ρ is the density and M_m is the monomeric molar mass

Luminescent polymer	Solvent	Sample length ℓ (μm)	Concentration C_{LP} (mol dm^{-3})
1,3-PPV 8	neat	0.071	1.72
	PS	2.5	0.078
	THF	1000	2.2×10^{-5}
1,3-PPV 10	neat	0.027	1.53
	PS	4.2	0.092
	THF	1000	7.9×10^{-5}
1,4-PPV 12/1	neat	0.11	1.43
	PS	1.7	0.055
	THF	1000	6.8×10^{-5}
PBV-PPV 1,10	neat	0.5	2.05
	PS	6.2	0.14
	THF	1000	1.3×10^{-3}
OPP	neat	0.089	1.48
	PS	6.16	0.039
	THF	1000	7.2×10^{-4}
OPT	neat	0.094	1.36
	PS	1.7	0.15
	THF	1000	4.8×10^{-5}

Data of ρ are given in [34].

polymers, otherwise the random walk polymer chains would shrink to globules [51] and a strong polymer segment–polymer segment interaction within the globules would be expected.

The spectral fluorescence structure (Fig. 5) of the luminescent polymers in liquid solution was identified as being due to emission from different lattice relaxed excited state conformations [26–28]. The more pronounced spectral broadening and spectral structuring of the luminescent polymers in polystyrene and in neat films is thought to be also due to fast polymer segment relaxation to less energetic conformations and emission from a variety of conformationally different sites.

In Fig. 5(e), $E_F(\lambda)$ of diluted OPP in polystyrene is included by a dotted curve (fluorescence quantum yield, $\phi_F = 0.29$). The spectral distribution lies between the distributions belonging to diluted OPP in THF and to concentrated OPP in polystyrene. The enhanced broadening in highly doped films and neat films is thought to be due to the nearby polymer chain–polymer chain interaction and structuring.

The fluorescence lifetimes of the investigated luminescent polymers (Table 2) fall by a factor of 1.2 to 3.3 in going from liquid solutions to blended films of rather high luminescent polymer doping (doping listed in Table 3). A considerable drop in fluorescence lifetime is observed in going from liquid solution to neat thin films for all investigated polymers with the exception of PBV-PPV 1,10. For PBV-PPV 1,10 the fluorescence quantum yield of neat films is only reduced by a factor of 1.8 compared to liquid THF solutions. Travelling-wave lasing was achieved with PBV-PPV 1,10 neat thin films [25].

The wavelength dependence of the degree of fluorescence polarisation is displayed in Fig. 6 for the investigated polymers in neat films, blended films and THF solutions. For an isotropic distribution of absorbing chromophores and excitation by electric dipole interaction, the degree of fluorescence polarisation (Eq. (5)) is limited to between $-0.33 \le P_F(\lambda) \le 0.5$ [42]. Values of P_F near 0.5 are expected if the absorbing and emitting transition dipole moments are parallel to one another and there occurs no reorientation of the emitting transition dipole moments within the fluorescence lifetime. Values of P_F near -0.33 are expected when the absorbing and emitting transition dipole moments are oriented perpendicular to one another and there occurs no reorientation of the emitting transition dipole moments within the fluorescence lifetime. If the emitting transition

dipole moments reorient quickly compared to the fluorescence lifetime, then degrees of fluorescence polarisation of P_F near 0 are expected. A reorientation of the emitting transition dipole moments may occur by chromophore reorientation (emitting part within polymer chain or polymer segment [26,27]) or by excitation transfer to another differently oriented chromophore (intra-chain excitation transfer to differently oriented polymer segments of a polymer chain, and inter-chain excitation transfer in highly concentrated blended films and neat films [29,49,50]). Wavelength dependent changes of the degree of fluorescence polarisation indicate different orientations of different emitting chromophores. Stiff backbone polymers are expected to have a higher degree of fluorescence polarisation than flexible chain polymers (excitation transfer to segments of the same orientation).

For a fixed transition dipole moment reorientation time, τ_{or}, the degree of fluorescence polarisation, P_F, is the larger the shorter the fluorescence lifetime, τ_F (less time available for reorientation before deactivation). The calculated monomeric transition dipole moment reorientation times listed in Table 1 are shortest for the neat films and longest for the diluted THF solutions, while the polymer segment reorientation time should be shortest in liquid solution. This finding indicates that the fluorescence depolarisation is dominated by chromophore–chromophore energy transfer, which is highest in neat films.

The actual degree of fluorescence polarisation as a function of wavelength of the investigated luminescent polymers (Fig. 6) is determined by a complex interplay between polymer segment alignment and reorientation, conformational distribution, excitation transfer, and fluorescence lifetime.

High fluorescence quantum yields are important for laser action. Amplified spontaneous emission was achieved in PBV-PPV 1,10 neat and blended films which have high fluorescence quantum yields [25]. High neat-film fluorescence quantum yields were reported for other luminescent polymers which showed neat film laser action [12,24,30].

In contrast to some luminescent polymer films, in neat films of common organic laser dyes the fluorescence quantum yield is generally quenched severely hindering laser action. As an example, for a neat rhodamine 6G film [52] we obtained only a fluorescence quantum yield of $\phi_F \approx 2 \times 10^{-3}$. For comparison, the fluorescence quantum distribution spectrum of a neat rhodamine 6G film is included in Fig. 5(f) (dotted curve). The dye–dye interaction efficiently quenches the fluorescence emission. Quite recently, however, amplified spontaneous emission in neat thin films consisting of some spiro-type small molecules has been achieved [53], indicating a high fluorescence quantum yield of these molecules in the solid state.

Light amplification in lasing devices depends on the effective stimulated emission cross-section, $\sigma_{em,eff}(\lambda) = \sigma_{em}(\lambda) - \sigma_{ex}(\lambda)$. An evaluation of the lasing performance of the neat and blended luminescent polymer films requires measurements of the excited-state absorption cross-section spectra, $\sigma_{ex}(\lambda)$. These measurements are outside the scope of the present paper (excited state absorption studies on liquid solutions of 1,3-PPV 8, OPP and OPT were performed earlier [26,27]). The presented stimulated emission cross-section spectra show the regions of possible laser action in the case of favorably small excited-state absorption ($\sigma_{ex,m}(\lambda) < \sigma_{em,m}(\lambda)$).

5. Conclusions

The fluorescence spectroscopic behaviour of six luminescent polymers in neat films and blended polystyrene films was investigated. The thin film results have been compared with the corresponding results in liquid tetrahydrofuran solution. The investigated luminescent polymers were previously used for laser action in liquid solutions [7,8] and are potential candidates for laser action in neat and doped solid films [25].

The fluorescence quantum efficiency of the investigated neat films reduces to the 2–5% region. However, there is one exception (PBV-PPV 1,10) with a fluorescence quantum yield of about 40%, which shows that molecular engineering is able to build luminescent polymers with high fluorescence efficiency in undiluted solid state. A detailed understanding why the fluorescence quenching in solid PBV-PPV 1,10 is strongly reduced compared to the other investigated compounds is still missing. For some other luminescent polymers, high neat

film fluorescence quantum efficiencies were reported [12,21,24]. The highly concentrated luminescent polymers in polystyrene thin films investigated here have rather high fluorescence quantum yields only approximately a factor of 1.2 to 4.1 below the efficiency of diluted liquid solutions.

The fluorescence spectra of the investigated neat and highly doped blended thin films are remarkably broadened and long-wavelength shifted compared to the diluted liquid solutions, indicating a strong inter-polymer interaction and the emission from different lattice relaxed structured conformations. While the studied luminescent polymers have liquid solution fluorescence emission peaks in the violet and blue spectral region, the fluorescence bands of the neat and blended films are in the green region and extend to the yellow, orange and red region. The broad spectral emission regions make the studied luminescent polymers attractive candidates for broadly tunable lasers.

Acknowledgements

We thank the Commission of the European Union for support under the ESPRIT LTR Project Program LUPO: Project No 28580. We thank E. Drotleff for initial assistance in fluorescence measurements and we are indebted to Professor D. Weiss for allowing use to the Dektak 3 stylus profilometer.

Appendix A. Fluorescence analysis

The fluorescence signal measurement for liquid solutions and thin films on transparent substrates (indicated by index F) and for reference dye solution samples (indicated by index R) are carried out with the same excitation source of input energy, W_L, and frequency, ν_L. The fluorescence quantum distribution, $E_F(\lambda)$, is defined by

$$E_F(\lambda) = \frac{S_i(\lambda)}{S_{abs}} = \frac{4\pi s_i(\lambda)}{S_{abs}} = \frac{4\pi s_i(\lambda) h\nu_L}{W_L(1 - R_L - T_L)}, \tag{A1}$$

where $S_I(\lambda)$ is the intrinsic spectral fluorescence photon density distribution, $s_i(\lambda)$ is the angular averaged intrinsic spectral fluorescence photon density distribution per steradiant, S_{abs} is the total number of absorbed excitation photons, R_L is the reflectance, and T_L is the transmittance of the excitation light.

The fluorescence quantum yield, ϕ_F, is defined by

$$\phi_F = \int_{em} E_F(\lambda)\mathrm{d}\lambda. \tag{A2}$$

The fluorescence quantum yield, ϕ_R, of the reference dye is known. The fluorescence quantum yield, ϕ_F, of the luminescent polymer sample has to be determined.

The relation between ϕ_F and ϕ_R is found by use of Eq. (A1) and (A2) to be

$$\phi_F = \frac{\int_{em} S_{I,F}(\lambda)\mathrm{d}\lambda}{\int_{em} S_{I,R}(\lambda)\mathrm{d}\lambda} \frac{W_{L,R}(1 - R_{L,R} - T_{L,R})}{W_{L,F}(1 - R_{L,F} - T_{L,F})} \phi_R = \frac{\int s_{I,F}(\lambda)\mathrm{d}\lambda}{\int s_{I,R}(\lambda)\mathrm{d}\lambda} \frac{W_{L,R}(1 - R_{L,R} - T_{L,R})}{W_{L,F}(1 - R_{L,F} - T_{L,F})} \phi_R. \tag{A3}$$

The fluorescence quantum distribution, $E_F(\lambda)$, is given by

$$E_F(\lambda) = \frac{S_{I,F}(\lambda)}{\int_{em} S_{I,R}(\lambda)\mathrm{d}\lambda} \frac{W_{L,R}(1 - R_{L,R} - T_{L,R})}{W_{L,F}(1 - R_{L,F} - T_{L,F})} \phi_R = \frac{s_{I,F}(\lambda)}{\int_{em} s_{I,R}(\lambda')\mathrm{d}\lambda'} \frac{W_{L,R}(1 - R_{L,R} - T_{L,R})}{W_{L,F}(1 - R_{L,F} - T_{L,F})} \phi_R. \tag{A4}$$

In the experiments, the spectral fluorescence signal distributions, $S_m(\lambda)$, of the sample (F) and the reference (R) are measured by a diode-array detection system behind a spectrometer (signal height is proportional to detected fluorescence photons). For the determination of $E_F(\lambda)$ and ϕ_F relations between $S_m(\lambda)$ and $s_I(\lambda)$ have to be found for the sample under investigation (F) and the reference sample (R). These relations are developed reasonably accurately in the following including fluorescence absorption, re-emission, transmission and reflection. In thin films the lateral film region imaged to the spectrometer entrance slit is large compared to the film thickness. The lateral fluorescence emission in waveguiding and non-waveguiding thin films is absorbed and leads to enhanced subsequent fluorescence emission into the direction of the detection system. This enhanced fluorescence detection is taken into account.

The relation between $S_m(\lambda)$ and $s_I(\lambda)$ for front-face fluorescence collection (see Fig. 2) is given by

$$S_m(\lambda) = T_{det}(\lambda)\frac{\Delta\Omega_{det}}{n^2(\lambda)}\left[s_0(\lambda) + s_{\swarrow}(\lambda)R_{\swarrow}(\lambda)T'(\lambda)\right]\frac{1-R_0(\lambda)}{1-T'^2(\lambda)R_{\swarrow}(\lambda)R_0(\lambda)}f_{re}, \tag{A5}$$

where $T_{det}(\lambda)$ is the transmission factor of the fluorescence signal from just outside the sample to the spectrometer and through the spectrometer including the detector sensitivity, $\Delta\Omega_{det}$ is the solid acceptance angle of the detection system outside the sample, the internal solid acceptance angle (inside the sample) is $\Delta\Omega_I(\lambda) = \Delta\Omega_{det}/n^2(\lambda)$ and it is reduced due to refraction at the border between sample and air, $s_0(\lambda)$ is the angular averaged intrinsic spectral fluorescence photon density per steradiant inside the entrance surface corrected for absorption and re-emission, and $s_{\swarrow}(\lambda)$ is the angular averaged intrinsic spectral fluorescence photon density per steradiant inside the exit surface corrected for absorption and re-emission. The angular averaging is achieved by linear polarised excitation and linear polarised magic-angle fluorescence detection (fluorescence polariser at angle of 54.74° to excitation polariser). The factor $R_{\swarrow}(\lambda)T'(\lambda)$ gives the fraction of $s_{\swarrow}(\lambda)$ which adds to $s_0(\lambda)$ at the entrance surface position. $R_{\swarrow}(\lambda) \approx (n_{\swarrow}-1)^2/(n_{\swarrow}+1)^2$ is the reflectance at the exit surface, where $n_{\swarrow}$ is the refractive index of the exit material (e.g. substrate or cell window), $T'(\lambda) = \exp[-\sigma_{a,m}(\lambda)N_m\swarrow]$ is the neat transmission through the sample, $\sigma_{a,m}(\lambda)$ is the monomeric absorption cross-section at wavelength λ, and N_m is the monomeric number density of fluorescing molecules. The nominator $[1-R_0(\lambda)]$ gives the transmittance of the entrance surface, and the denominator $[1-T'(\lambda)R_{\swarrow}(\lambda)R_0(\lambda)]$ takes care of multiple reflections and transmissions. $R_0(\lambda) \approx (n_0-1)^2/(n_0+1)^2$ is the reflectance of the entrance surface, where n_0 is the refractive index of the entrance medium (e.g. thin film or cell window). f_{re} is the enhancement factor of the detected fluorescence signal due to re-emission of absorbed fluorescence light.

At a position x inside the sample, the contribution to the intrinsic spectral fluorescence photon density is [39]

$$\frac{ds_I(\lambda,x)}{dx} = \frac{ds_I(\lambda,0)}{dx}\exp(-N_m\sigma_{L,m}x). \tag{A6}$$

Integration of Eq. (A6) over the sample length gives

$$s_I(\lambda) = \frac{ds_I(\lambda,0)}{dx}\frac{1-T'_L}{N_m\sigma_{L,m}}. \tag{A7}$$

The contribution to $s_0(\lambda)$ from the emission $ds_I(\lambda,x)/dx$ at position x is

$$\frac{ds_0(\lambda,x)}{dx} = \frac{ds_I(\lambda,x)}{dx}\exp(-N_m\sigma_{a,m}(\lambda)x) = \frac{ds_I(\lambda,0)}{dx}\exp\left[-N_m(\sigma_{L,m}+\sigma_{a,m}(\lambda))x\right]. \tag{A8}$$

Integration of Eq. (A8) over the sample length gives

$$s_0(\lambda) = \frac{\mathrm{d}s_I(\lambda,0)}{\mathrm{d}x}\,\frac{1-\exp\left[-N_m x(\sigma_{L,m}+\sigma_{a,m}(\lambda))\right]}{N_m\left[\sigma_{L,m}+\sigma_{a,m}(\lambda)\right]} \tag{A9a}$$

$$s_0(\lambda) = s_I(\lambda)\,\frac{\sigma_{L,m}}{\sigma_{L,m}+\sigma_{a,m}(\lambda)}\,\frac{1-T_L'^{\,[\sigma_{L,m}+\sigma_{a,m}(\lambda)]/\sigma_{L,m}}}{1-T_L'} \tag{A9b}$$

$$s_0(\lambda) = s_I(\lambda)\,A(\lambda). \tag{A9c}$$

Eq. (A9b) is obtained from Eq. (A9a) by insertion of Eq. (A7). In Eq. (A9c), an abbreviation $A(\lambda)$ is defined.

The contribution to $s_\ell(\lambda)$ from position x is

$$\frac{\mathrm{d}s_\ell(\lambda,x)}{\mathrm{d}x} = \frac{\mathrm{d}s_I(\lambda,x)}{\mathrm{d}x}\exp\left[-N_m\sigma_{a,m}(\lambda)(\ell-x)\right] \tag{A10a}$$

$$\frac{\mathrm{d}s_\ell(\lambda,x)}{\mathrm{d}x} = \frac{\mathrm{d}s_I(\lambda,0)}{\mathrm{d}x}\exp(-N_m\sigma_{L,m}x)T'(\lambda)\exp\left(N_m\sigma_{a,m}(\lambda)x\right) \tag{A10b}$$

$$\frac{\mathrm{d}s_\ell(\lambda,x)}{\mathrm{d}x} = \frac{\mathrm{d}s_I(\lambda,0)}{\mathrm{d}x}T'(\lambda)\exp\left\{-N_m x\left[\sigma_{L,m}-\sigma_{a,m}(\lambda)\right]\right\}. \tag{A10c}$$

Eq. (A10b) is obtained by insertion of Eq. (A6) into Eq. (A10a).

Integration of Eq. (A10c) over the sample length results in

$$s_\ell(\lambda) = \frac{\mathrm{d}s_I(\lambda,0)}{\mathrm{d}x}T'(\lambda)\,\frac{1-T_L'/T'(\lambda)}{N_m\left[\sigma_{L,m}-\sigma_{a,m}(\lambda)\right]} \tag{A11a}$$

$$s_\ell(\lambda) = \frac{\mathrm{d}s_I(\lambda,0)}{\mathrm{d}x}\,\frac{T'(\lambda)-T_L'}{N_m\left[\sigma_{L,m}-\sigma_{a,m}(\lambda)\right]} \tag{A11b}$$

$$s_\ell(\lambda) = s_I(\lambda)\,\frac{\sigma_{L,m}}{\sigma_{L,m}-\sigma_{a,m}(\lambda)}\,\frac{T'(\lambda)-T_L'}{1-T_L'} \tag{A11c}$$

$$s_\ell(\lambda) = s_I(\lambda)\,B(\lambda). \tag{A11d}$$

Eq. (A11c) is obtained from Eq. (A11b) by insertion of Eq. (A7). In Eq. (A11d), an abbreviation $B(\lambda)$ is defined.

Up to now, re-emission of absorbed fluorescence light has been neglected. The re-emission of absorbed fluorescence light increases the measured fluorescence signal, $S_m(\lambda)$, by a factor of f_{re}. Re-emission within the sample volume $\ell \times d \times h$ contributes, where ℓ is the sample thickness, d is the imaged spectrometer slit width ($d = d_{slit}\ f_3/f_4$, where f_3 and f_4 are the focal lengths of lenses L3 and L4 in Fig. 2), and h is the imaged diode-array sensor height at the sample ($h > d$). Cross-sections through the fluorescing samples are shown in Fig. 2(b) and Fig. 2(c). Within the angle φ_{esc} ($\varphi_{esc} = \varphi_m$ in non-waveguiding samples; $\varphi_{esc} = \varphi_t$ in waveguiding samples) fluorescent rays escape from the front and end faces of the sample. The average path length is $\ell/[2\cos(\varphi)]$. In the angular region between φ_{esc} and $\pi/2$, the fluorescence rays remain inside the imaged volume. The path length is approximately given by $\tilde{d} = (d \times h)^{1/2}$.

In an approximate way, f_{re} is given by

$$f_{re} = 1 + (1-\tilde{T})\,\phi_F + \left[(1-\tilde{T})\,\phi_F\right]^2 + \cdots \tag{A12a}$$

$$f_{re} = \frac{1}{1-(1-\tilde{T})\,\phi_F} \tag{A12b}$$

$$f_{re} < \frac{1}{1-\phi_F}, \tag{A12c}$$

where $\tilde{T}$ is the averaged fluorescence transmission. It is approximately given by

$$\tilde{T} = \frac{\int_{em} s_i(\lambda)\left\{\int_0^{\varphi_{esc}} \exp\left[-\frac{\sigma_{a,m}(\lambda) N_m \ell}{2\cos(\varphi)}\right]\sin(\varphi)\,d\varphi + \exp\left[-\sigma_{a,m}(\lambda) N_m \tilde{d}\right]\cos(\varphi_{esc})\right\}d\lambda}{\int_{em} s_i(\lambda)\,d\lambda}. \quad (A13)$$

The integral in the curly brackets covers the transmission of rays in the angular region between 0 and φ_{esc}. The second term in the curly brackets covers the fluorescence transmission within the angular region φ_{esc} to $\pi/2$.

For non-waveguiding bulk samples and non-waveguiding thin films φ_{esc} is given by

$$\varphi_{esc} = \varphi_m = \arctan\left(\tilde{d}/\ell\right), \quad (A14a)$$

while for waveguiding thin film samples φ_{esc} is given by

$$\varphi_{esc} = \min(\varphi_m, \varphi_t), \quad (A14b)$$

where

$$\varphi_t = \arcsin\left(\frac{n_s}{n_f}\right) \quad (A14c)$$

is the angle of total internal reflection, and n_s and n_f are the average refractive indices of the substrate and the film in the fluorescence region, respectively. Waveguiding occurs if [55]

$$n_f > n_s \quad (A15a)$$

and

$$\ell > \ell_{crit} = \frac{\lambda_F}{2\pi\left(n_f^2 - n_s^2\right)^{1/2}} \arctan\left(\frac{n_s^2 - 1}{n_f^2 - n_s^2}\right)^{1/2}. \quad (A15b)$$

The wavelength λ_F is approximately equal to the wavelength of peak fluorescence emission.

For the investigated neat films and blended films, the values of λ_F, n_f, n_s, φ_t, φ_{esc}, ℓ_{crit}, and ℓ are collected in Table 4 ($d = 0.65$ mm, $h = 1.8$ mm. $\tilde{d} \approx 1$ mm). The neat films except PBV-PPV 1,10 are not waveguiding because $\ell < \ell_{crit}$. All blended films are waveguiding.

Table 4
Waveguiding data of investigated luminescent polymer films

Sample		λ_F (nm)	n_f	n_s	φ_t (°)	ℓ_{crit} (nm)	ℓ (nm)	φ_{esc} (°)
1,3-PPV 8	neat	502	1.687	1.462	60.07	85.7	71	89.99
	PS	502	1.604	1.462	65.70	123.1	2500	65.70
1,3-PPV 10	neat	488	1.600	1.463	66.12	123.0	27	90.00
	PS	502	1.604	1.462	65.70	123.1	4200	65.71
1,4-PPV 12/1	neat	548	1.795	1.4598	54.42	66.3	110	89.99
	PS	517	1.601	1.4608	65.84	12.8	1700	65.84
PBV-PPV 1,10	neat	466	1.628	1.464	64.06	102.4	500	64.06
	PS	443	1.615	1.4663	65.22	105.0	6200	65.22
OPP	neat	587	1.639	1.4598	62.96	120.3	89	89.99
	PS	453	1.613	1.4653	65.29	107.9	6160	65.29
OPT	neat	556	1.649	1.4598	62.28	109.2	94	89.99
	PS	479	1.608	1.464	65.57	116.3	1700	65.57

Imaged lateral sample extension $\tilde{d} \approx 1$ mm.

Eq. (A12c) shows that for weakly fluorescing samples ($\phi_F \ll 1$) fluorescence re-emission may be neglected. Eq. (A13) indicates that for bulk samples with $\ell \gg \tilde{d}$ and reasonable pump pulse transmission ($T'_L > 0.1$) fluorescence reabsorption is small.

Inserting Eqs. (A9c) and (A11d) into Eq. (A5) and solving for $s_I(\lambda)$ one obtains for the intrinsic spectral fluorescence photon density per steradiant of the reference sample, $s_{I,R}(\lambda)$, and of the sample under investigation, $s_{I,F}(\lambda)$, the following expressions

$$s_{I,R}(\lambda) = S_{m,R}(\lambda)\frac{n_R^2(\lambda)}{\Delta\Omega_{det}}\frac{1-T_R'^2(\lambda)R_{\ell,R}(\lambda)R_{0,R}(\lambda)}{1-R_{0,R}(\lambda)}\frac{1}{T_{det}(\lambda)f_{re,R}}\frac{1}{A_R(\lambda)+B_R(\lambda)R_{\ell,R}(\lambda)T'_R(\lambda)} \tag{A16}$$

and

$$s_{I,F}(\lambda) = S_{m,F}(\lambda)\frac{n_F^2(\lambda)}{\Delta\Omega_{det}}\frac{1-T_F'^2(\lambda)R_{\ell,F}(\lambda)R_{0,F}(\lambda)}{1-R_{0,F}(\lambda)}\frac{1}{T_{det}(\lambda)f_{re,F}}\frac{1}{A_F(\lambda)+B_F(\lambda)R_{\ell,F}(\lambda)T'_F(\lambda)}. \tag{A17}$$

The insertion of Eqs. (A16) and (A17) into Eqs. (A3) and (A4) allows the calculation of ϕ_F and $E_F(\lambda)$ from measured quantities. Since $f_{re,F}$ depends on ϕ_F, Eqs. (A3) (ϕ_F) and (A4) ($E_F(\lambda)$) can be solved only iteratively assuming a start value of ϕ_F in the expression of $f_{re,F}$ for the first iteration. If ϕ_F is small, the re-emission factor may be neglected (see Eq. (A12c)).

References

[1] N.C. Greenham, R.H. Friend, in: H. Ehrenreich, F. Spaepen (Eds.), Solid State Physics, vol. 49, Academic Press, San Diego, 1995, p. 2.
[2] J.E. Mark (Ed.), Physical Properties of Polymers Handbook, American Institute of Physics, New York, 1996.
[3] A.J. Heeger, J. Long, Optics and Photonics News, August 1996, p. 27.
[4] N. Tessler, N.T. Harrison, R.H. Friend, Adv. Mater. 10 (1998) 64.
[5] D. Moses, Appl. Phys. Lett. 60 (1992) 3215.
[6] H.J. Brouwer, V.V. Krasnikov, A. Hilberer, J. Wildeman, G. Hadziioannou, Appl. Phys. Lett. 66 (1995) 3404.
[7] W. Holzer, A. Penzkofer, S.-H. Gong, A. Bleyer, D.D.C. Bradley, Adv. Mater. 8 (1996) 974.
[8] W. Holzer, A. Penzkofer, S.-H. Gong, W.J. Blau, A.P. Davey, Opt. Quant. Electron. 29 (1997) 713.
[9] N.D. Kumar, J.D. Bhawalkor, P.N. Prasad, F.E. Karasz, B. Hu, Appl. Phys. Lett. 71 (1997) 999.
[10] G. Wegmann, H. Giessen, D. Hertel, R.F. Mahrt, Solid State Commun. 104 (1997) 759.
[11] F. Hide, B.J. Schwartz, M.A. Díaz-García, A.J. Heeger, Chem. Phys. Lett. 256 (1996) 424.
[12] M.A. Díaz-García, F. Hide, B.J. Schwartz, M.D. McGehee, M.R. Andersson, A.J. Heeger, Appl. Phys. Lett. 70 (1997) 3191.
[13] N. Tessler, G.J. Denton, R.H. Friend, Nature 382 (1996) 695.
[14] A. Schülzgen, Ch. Spiegelberg, M.M. Morrell, S.B. Mendes, M.F. Nabot, E.A. Mash, P.M. Allemand, B. Kippelen, N. Peyghambarian, CLEO'98 Conference on Lasers and Electro-Optics, 1998, Technical Digest Series, vol. 6, CBB2, May 3–8, 1998, pp. 6–7.
[15] M. McGehee, R. Hick, M. Díaz-García, B.J. Schwartz, D. Moses, A.J. Heeger, presented at Materials Research Society, Spring 1997 Meeting, San Francisco, CA, April 1997.
[16] C. Kallinger, M. Hilmer, A. Haugeneder, M. Perner, W. Spirkl, U. Lemmer, F. Feldmann, U. Scherf, K. Müllen, A. Gombert, V. Wittwer, Adv. Mater. 10 (1998) 920.
[17] F. Hide, M.A. Díaz-García, B.J. Schwartz, M.R. Andersson, Q. Pei, A.J. Heeger, Science 273 (1996) 1833.
[18] H.J. Brouwer, V.V. Krasnikov, A. Hilberer, G. Hadziioannou, Adv. Mater. 8 (1996) 935.
[19] C. Zens, W. Gaupner, S. Tasch, G. Leising, K. Müllen, U. Scherf, Appl. Phys. Lett. 71 (1997) 2566.
[20] S.V. Frolov, M. Ozaki, W. Gellermann, Z.V. Vardeny, K. Yoshino, Jpn. J. Appl. Phys. 35 (1996) L1371.
[21] S.V. Frolov, W. Gellermann, M. Ozaki, K. Yoshino, Z.V. Vardeny, Phys. Rev. Lett. 78 (1997) 729.
[22] G.J. Denton, N. Tessler, M.A. Stevens, R.H. Friend, Adv. Mater. 9 (1997) 547.
[23] A. Haugeneder, M. Hilmer, C. Kallinger, M. Perner, W. Spirkl, U. Lemmer, J. Feldmann, U. Scherf, Appl. Phys. B 66 (1998) 389.
[24] G.H. Gelnick, J.M. Warman, M. Remmers, D. Neher, Chem. Phys. Lett. 256 (1997) 320.

[25] A. Penzkofer, W. Holzer, S.-H. Gong, D.D.C. Bradley, X. Long, A. Bleyer, W.J. Blau, A.P. Davey, Lasing Studies of Luminescent Polymers, Proceed. of Int. Conference on LASERS'98, Tucson, AZ, USA, Dec. 7–11, in press.
[26] W. Holzer, A. Penzkofer, S.-H. Gong, D.D.C. Bradley, X. Long, A. Bleyer, Chem. Phys. 224 (1997) 315.
[27] W. Holzer, A. Penzkofer, S.-H. Gong, W.J. Blau, A.P. Davey, Opt. Quant. Electron. 30 (1998) 1.
[28] W. Holzer, A. Penzkofer, S.-H. Gong, D.D.C. Bradley, X. Long, W.J. Blau, A.P. Davey, Polymer 39 (1998) 3651.
[29] Th. Förster, Fluoreszenz organischer Verbindungen, Vandenhoeck und Ruprecht, Göttingen, 1951.
[30] N.C. Greenham, I.D.W. Samuel, G.R. Hayes, R.T. Phillips, Y.A.R.R. Kessener, S.C. Moratti, A.B. Holmes, R.H. Friend, Chem. Phys. Lett. 241 (1995) 89.
[31] D. Braun, E.G.J. Staring, R.C.J.E. Demandt, G.L.J. Rikken, Y.A.R.R. Kessener, A.H.J. Venhuizen, Synth. Metals 66 (1994) 75.
[32] E.G.J. Staring, R.C.J.E. Demandt, D. Braun, G.L.J. Rikken, Y.A.R.R. Kessener, T.H.J. Venhuizen, H. Wynberg, W. ten Hoeve, K.J. Spoelstra, Adv. Mater. 6 (1994) 934.
[33] A.P. Davey, S. Elliott, O. O'Connor, W.J. Blau, J. Chem. Soc. Chem. Commun., 1995, 1433.
[34] W. Holzer, M. Pichlmaier, E. Drotleff, A. Penzkofer, D.D.C. Bradley, W.J. Blau, Opt. Commun. 163 (1999) 24.
[35] M. Born, E. Wolf, Principles of Optics. Electromagnetic Theory of Propagation, Interference and Diffraction of Light, 6th ed., Pergamon Press, Oxford, 1980.
[36] D.E. Gray (Ed.), American Institute of Physics Handbook, 3rd ed., McGraw-Hill, New York, 1972.
[37] J.B. Birks, Photophysics of Aromatic Molecules, Wiley, London, 1970, p. 51.
[38] N.J. Turro, Modern Molecular Photochemistry, Benjamin/Cummings Publishing, Menlo Park, CA, 1978, p. 86.
[39] A. Penzkofer, W. Leupacher, J. Luminesc. 37 (1987) 61.
[40] R. Lakowicz, Principles of Fluorescence Spectroscopy, Plenum Press, New York, 1983.
[41] Technical data sheet Coumarin 314 T of Kodak, Rochester, New York 14652–3512.
[42] F. Dörr, Angew. Chemie 78 (1966) 457.
[43] E.D. Cehelnik, K.C. Mielenz, R.A. Velapoldi, J. Research Nat. Bureau of Standards - A, Physics and Chemistry 79A (1971) 991.
[44] O.G. Peterson, J.P. Webb, W.C. McColgin, J.H. Eberly, J. Appl. Phys. 42 (1971) 1917.
[45] S.J. Strickler, R.A. Berg, J. Chem. Phys. 37 (1962) 814.
[46] J.B. Birks, D.J. Dyson, Proc. Roy. Soc. London, Ser. A 275 (1963) 135.
[47] G. Weber, in: D.M. Hercules (Ed.), Fluorescence and Phosphorescence Analysis, Principles and Applications, Interscience, New York, 1966, p. 217.
[48] P. Weidner, A. Penzkofer, Chem. Phys. 191 (1995) 303.
[49] Th. Förster, in: O. Sinanoglu (Ed.), Modern Quantum Chemistry, Part III, Academic Press, New York, 1965, p. 93.
[50] G.R. Fleming, Chemical Applications of Ultrafast Spectroscopy, Oxford University Press, New York, 1986.
[51] M. Doi, Introduction to Polymer Physics, Clarendon Press, Oxford, 1996.
[52] A. Penzkofer, E. Drotleff, W. Holzer, Opt. Commun. 158 (1998) 221.
[53] N. Johansson, J. Salbeck, J. Bauer, F. Weissörtel, P. Bröms, A. Andersson, W.R. Salaneck, Adv. Mater. 10 (1998) 1136.
[54] A. Penzkofer, H. Glas, J. Schmailzl, Chem. Phys. 70 (1982) 47.
[55] H. Kogelnik, Integrated optics, in: T. Tamir (Ed.), Topics in Applied Physics, vol. 7, Springer-Verlag, Berlin, 1979, p. 13.